Molecules and Cells

E3 ligase BRUTUS Is a Negative Regulator for the Cellular Energy Level and the Expression of Energy Metabolism-Related Genes Encoded by Two Organellar Genomes in Leaf Tissues

Bongsoo Choi[1], Do Young Hyeon[2], Juhun Lee[1], Terri A. Long[4], Daehee Hwang[2,3], and Inhwan Hwang[1,*]

[1]Department of Life Science, Pohang University of Science and Technology, Pohang 37673, Korea, [2]School of Biological Sciences, Seoul National University, Seoul 08826, Korea, [3]Bioinformatics Institute, Seoul National University, Seoul 08826, Korea, [4]Department of Plant and Microbial Biology, North Carolina State University, Raleigh, NC 27695, USA
*Correspondence: ihhwang@postech.ac.kr
https://doi.org/10.14348/molcells.2022.2029
www.molcells.org

E3 ligase BRUTUS (BTS), a putative iron sensor, is expressed in both root and shoot tissues in seedlings of *Arabidopsis thaliana*. The role of BTS in root tissues has been well established. However, its role in shoot tissues has been scarcely studied. Comparative transcriptome analysis with shoot and root tissues revealed that *BTS* is involved in regulating energy metabolism by modulating expression of mitochondrial and chloroplast genes in shoot tissues. Moreover, in shoot tissues of *bts-1* plants, levels of ADP and ATP and the ratio of ADP/ATP were greatly increased with a concomitant decrease in levels of soluble sugar and starch. The decreased starch level in *bts-1* shoot tissues was restored to the level of shoot tissues of wild-type plants upon vanadate treatment. Through this study, we expand the role of *BTS* to regulation of energy metabolism in the shoot in addition to its role of iron deficiency response in roots.

Keywords: *Arabidopsis thaliana*, BRUTUS, energy metabolism, shoot tissues

INTRODUCTION

Iron is an essential mineral for all living organisms. Existing in multiple oxidation states, iron acts as a cofactor for many critical enzymes involved diverse biological processes (Kroh and Pilon, 2020; Lee et al., 2012b). On the other hand, excess Fe ions cause the formation of damaging reactive oxygen species (Kaplan and Ward, 2013). Plants therefore have mechanisms to control iron uptake, translocation, assimilation, and bioavailability (Kroh and Pilon, 2019; Hossain et al., 2018; Kobayashi and Nishizawa, 2012). In *Arabidopsis thaliana,* BTS appears to be part of a sophisticated mechanism for plants to maintain iron homeostasis. *BTS* mutants are embryonic lethal (Kobayashi et al., 2019). *BTS* knockdown mutant (*bts-1*) plants exhibit an increase in iron accumulation and show a markedly activated rhizosphere acidification compared with Col-0 plants. *bts-1* plants also show an insensitive phenotype to root growth inhibition and leaf chlorosis during iron deficiency (Hindt et al., 2017; Kobayashi et al., 2019; Selote et al., 2015). *BTS* is an iron-deficiency-induced gene whose transcript level increases in response to iron deficiency. Interestingly, the protein stability of BTS is destabilized upon iron binding (Selote et al., 2015). Iron binds to BTS through three

Received 21 November, 2021; revised 16 December, 2021; accepted 26 December, 2021; published online 15 April, 2022

eISSN: 0219-1032

hemerythrin domains. Upon iron binding to these domains, BTS is destabilized at the protein level (Selote et al., 2015). Thus, BTS is repressed by iron. Moreover, BTS negatively regulates a specific subset of iron-deficiency-inducible genes, such as PYE (Hindt et al., 2017). Therefore, BTS is thought to be a negative regulator of the iron deficiency response. It has been proposed that upon iron deficiency, BTS is produced as a negative regulator together with those involved in iron uptake in order to prevent excess iron uptake that might happen due to over-activation of the uptake process in response to iron deficiency.

In response to iron deficiency, the overall expression of *BTS* increases in the shoot, stele in the root, and embryos (Hindt et al., 2017). Arabidopsis contains two *BTS* paralogs, *BTS LIKE1* (*BTSL1*) and *BTS LIKE2* (*BTSL2*), which are largely expressed in the root epidermis and cortex (Hindt et al., 2017). They are also regulated by the iron deficiency response. BTSL1 and BTSL2 interact with and cause degradation of FER-LIKE FE DEFICIENCY-INDUCED TRANSCRIPTION FACTOR (FIT), a positive regulator of iron deficiency response, to prevent excess iron import from the soil (Rodriguez-Celma et al., 2019). However, *BTS* is expressed in the stele and negatively regulates a subgroup of IVc-type bHLH transcription factors, AtbHLH034/104/105 (ILR3) (Kobayashi et al., 2019). Using this two-step mechanism, Arabidopsis protects against iron toxicity in the root (Kobayashi et al., 2019; Rodriguez-Celma et al., 2019).

In contrast to the role of BTS in the root, the role of BTS in maintaining iron homeostasis in the shoot remains elusive. Since iron is a critical cofactor for enzymes in electron transfer and chlorophyll biosynthesis, iron status in the shoot should be important for various reactions, such as photosynthesis in leaf tissues (Kobayashi et al., 2019). A number of studies show that the shoot has a mechanism to sense the level of iron and trigger a phloem-mobile signal that communicates status of iron in the shoot to the root (Grillet et al., 2018; Kobayashi and Nishizawa, 2014; Mendoza-Cózatl et al., 2014). Thus, it is possible that iron status in the shoot plays a role in the control of iron uptake in the root (Enomoto et al., 2007; García et al., 2013; Vert et al., 2003). However, the mechanism concerning iron homeostasis in leaf tissues may be different from that in root tissues. Because of this possible difference in iron homeostasis between leaf and root tissues, the physiological role of BTS in shoot tissues may be different from that in root tissues. In this study, we used transcriptional analysis to investigate BTS function in shoots. Our analysis demonstrated that the lower level of BTS in *bts-1* plants results in significant changes in the shoot transcriptome, and one of these is related to the increase in energy metabolism.

MATERIALS AND METHODS

Plant materials and growth condition

The T-DNA insertion line of *bts-1* (SALK_016526) plants was previously isolated (Long et al., 2010). Knock-down effect of the mutation in *bts-1* plants was confirmed (Supplementary Fig. S1). Arabidopsis seeds were sown on half-strength MS medium (1/2 MS) plates containing 2 mM MES (pH 5.7) and 0.8% agar without sucrose. These plates were incubated at 4°C in the dark, transferred to a growth chamber and further grown for additional 10 days. The growth chamber was set up with 70-80 μmol m^{-2} s^{-1} white light under the 16/8 h light/dark cycle at 22°C ± 1°C during the day and 16 °C ± 4°C during the night. To treat plants with iron deficiency, plants grown on normal plates (50 μM Fe^{+2}) for 3 days were transferred to the iron depleted (0 μM Fe^{+2}) or normal (50 μM Fe^{+2}) half-strength MS plates and further grown for additional 2 days.

Generation of transgenic plants

The binary construct *BpBΔHG* in the binary vector pCAMBIA was transformed into *bts-1* plants by the floral dipping method (Clough and Bent, 1998). Transgenic plants were screened on B5 plates supplemented with hygromycin (25 mg/L). T3 homo lines were selected and used in experiments.

Multiphoton microscopy

To acquire green flourescent protein (GFP) images of the leaves from 5-day-old plants (2 DAT, day after transfer to the iron deficiency condition), a multiphoton microscope (MPM) with a Ti-Sapphire laser (Chameleon Vision II; Coherent, Germary) was used at 140-fs pulse width and 80-MHz pulse repetition rate (TCS SP5 II; Leica). MPM images were acquired and processed by LAS AF Lite (Leica). The filter set had an excitation wavelength/spectral detection bandwidth of 930 nm/500 to 550 nm for GFP.

Preparation of the total protein extract and Western blot analysis

Total protein extracts were prepared as described previously with some modifications (Lee et al., 2021). Plant leaf tissues were ground in liquid nitrogen and homogenized using extraction buffer (50 mM Tris–HCl, pH 7.5, 150 mM NaCl, 1 mM EDTA, 0.1% Triton X-100, EDTA-free protease inhibitor cocktail [Roche, Switzerland]). The mixtures were centrifuged at 18,000 × *g* at 4°C for 10 min, and supernatants were collected as total soluble proteins. Concentration of total soluble proteins was measured using Bradford assay (Protein Assay Dye Reagent Concentrate; Bio-Rad, USA). Equal amount of total soluble proteins was separated by SDS-PAGE, and proteins were transferred to polyvinylidene difluoride (PVDF) membranes using semi-dry transfer (Hoefer, USA). Western blot analysis was carried out using anti-GFP antibody (1:2,000; Bioapp, Korea) and anti-tubulin beta chain (1:1,000; Agrisera, Sweden) antibodies. Chemifluorescence was detected using the Amersham Imager 680 system (GE Healthcare, USA).

Total RNA sequencing and transcriptome analysis

Total RNA was prepared from shoot tissues of Col-0 (wild-type) and *bts-1* (*bts-1*) plants grown on 1/2 MS plates without sucrose. Total RNA was isolated from leaf tissues using the Qiagen RNeasy mini kit (Qiagen, Germany) according to the manufacturer's instructions. RNA was treated with TURBO DNase (Invitrogen, USA). We constructed RNA-seq libraries using a NEXTflex Rapid Directional RNA-seq Kit (PerkinElmer, USA), following the manufacturer's instructions. The adaptor ligated libraries were sequenced using an

Illumina Hi-Seq 2500 (DNA Link, Korea). From the resulting read sequences for each sample, adapter sequences (TruSeq universal and indexed adapters) were removed using the cutadapt software (ver. 1.12) (Martin, 2011). The resulting reads were then aligned to the *Arabidopsis* reference genome (TAIR10) using TopHat aligner (ver. 2.1.0) (Trapnell et al., 2009) with the default options. After the alignment, we counted the mapped reads for gene features (GTF file of TAIR10) using HTSeq (Anders et al., 2015) (ver. 0.9.1) and calculated fragments per kilobase of transcript per million fragments mapped (FPKM) by dividing the mapped read counts by gene length and total number of reads mapped onto protein-coding genes. The raw and normalized data of mRNA-sequencing were deposited at the Gene Expression Omnibus database (GSE189090).

Identification of differentially expressed genes (DEGs)

The 'expressed' genes were first identified as the ones with FPKM larger than 1 in at least one sample. For those expressed genes, FPKM values were converted to $\log_2$-FPKM after adding one to the FPKM values. The $\log_2$-FPKMs were then normalized using the quantile normalization method (Bolstad et al., 2003). We then identified DEGs as the ones with absolute $\log_2$-fold-changes > 0.58 (1.5-fold) for the comparison of *bts-1* versus Col-0 plants. To identify cellular processes enriched by the DEGs, we performed the enrichment analysis of gene ontology biological processes (GOBPs) for the DEGs using DAVID software (Huang et al., 2009) and selected the GOBPs with *P* value < 0.05 as the processes enriched by the DEGs.

Quantitative real-time polymerase chain reaction (qRT-PCR)

Total RNA was isolated from leaf tissues using the Qiagen RNeasy mini kit according to the manufacturer's instructions. RNA was treated with TURBO DNase (Invitrogen). 2 μg of total RNA were converted into single-stranded cDNA using the high-capacity cDNA reverse transcription kit with random hexamer (Applied Biosystems, USA) (Wang et al., 2018). To perform qRT-PCR reactions, PowerUP SYBRGreen Master Mix (Applied Biosystems), cDNA and gene specific primers (Supplementary Table S1) were mixed, and PCR was performed using a cycling protocol of 15 s at 95°C and 60 s at 60°C for 40 cycles. *ACT2* was used as an internal control of qRT-PCR.

Measurement of ADP, ATP, NADPH, $NADP^+$, and contents of starch and soluble sugars

The level of ADP and ATP, and the ratio of ADP/ATP were measured by the ADP/ATP Ratio Assay Kit (MAK135; Sigma, USA) following the manufacturer's instruction. Luminescence was detected by the spectrophotometric multi-well plate reader (TECAN, Switzerland). The levels of NADPH, $NADP^+$ and the ratio of NADPH/$NADP^+$ were measured by NADP/NADPH Quantitation Kit (MAK038; Sigma) following the manufacturer's instruction. Optical density (OD) 450 nm was detected by spectrophotometric multi-well plate reader (TECAN). Total starch contents in shoot tissues were measured by the Starch Colorimetric/Fluorometric Assay Kit (BioVision, USA) following the manufacturer's instruction. OD 570 nm oxyred signal was detected by the spectrophotometric multi-well plate reader (TECAN). Soluble sugar content was measured by the CheKine™ Plant Soluble Sugar Colorimetric Assay Kit (KTB1320; Abbkine) following the manufacturer's instruction. OD 620 nm was detected by the spectrophotometric multi-well plate reader (TECAN).

IMAGING-PAM M-Series chlorophyll fluorescence system

The light induction curves of electron transport rate (ETR_{II}), effective quantum yield of PSII (Y_{II}) were measured by a Imaging-PAM chlorophyll fluorometer (Heinz Walz GmbH, Germany) as described previously (Li et al., 2021).

Measurement of chlorophyll contents

Chlorophyll contents were measured as described previously (Wang et al., 2018). Chlorophyll was extracted using 95% ethanol (v/v) from plant leaves at 4°C overnight in the dark. OD of extracted chlorophyll was measured at 664 nm and 648 nm to determine contents of chlorophyll a and b, respectively. The formula 5.24 × OD664/20 was used to calculate chlorophyll a contents and 22.24 × OD648/20 for chlorophyll b contents. Statistical analysis was performed using Student's *t*-test (GraphPad Prism 8 for Windows; GraphPad Software, USA). Values are mean ± SD (n = 3). A *P* value < 0.05 was considered statistically significant.

RESULTS

BTS is expressed in the leaf margin under normal conditions but induced in the entire leaf during iron deficiency

To elucidate the role of BTS in leaf tissues, we first examined the expression of *BTS* in the shoot of Arabidopsis. To monitor expression under a fluorescent microscope, we generated transgenic plants (BpBΔHGb) expressing *BΔHG* under the native promoter (*Bp*) in the background of the *bts-1* mutation. BΔHG had a deletion of the three hemerythrin domains of BTS (BΔH) and fusion of GFP at the C-terminus (Selote et al., 2015). The deletion of the three hemerythrin domains from BTS leads to an increase in the stability of BTS protein. *bts-1* plants have a 50% *BTS* expression level due to a T-DNA insertion at the 5' UTR region and do not respond to iron deficiency (Supplementary Fig. S1) (Hindt et al., 2017; Selote et al., 2015). The promoter region (*Bp*) consisted of a 3-kB *BTS* promoter genomic sequence. Using the BpBΔHGb plants, we examined the expression of *BΔHG* by the GFP fluorescent signal. Under a two-photon fluorescent microscope, we observed GFP signals where *BΔHG* was expressed. A GFP signal was observed at the leaf margin under normal growth conditions (50 μM Fe^{2+}) but was detected at much wider areas on the leaves upon iron deficiency (0 μM Fe^{2+}) treatment. Iron deficiency strongly induced the GFP signal in the entire area of leaves, resulting in a uniform expression of *BΔHG* in the leaf (Fig. 1A, 250×). The higher resolution image showed that the iron deficiency condition caused the expression of *BΔHG* in newly emerging leaves (arrows, Fig. 1B, 1,000×). To confirm the expression of *BΔHG* at the protein level, total protein extracts from BpBΔHGb plants were separated by SDS-PAGE and analyzed by western blotting using an anti-GFP antibody. Consistent with the image results, BΔHG

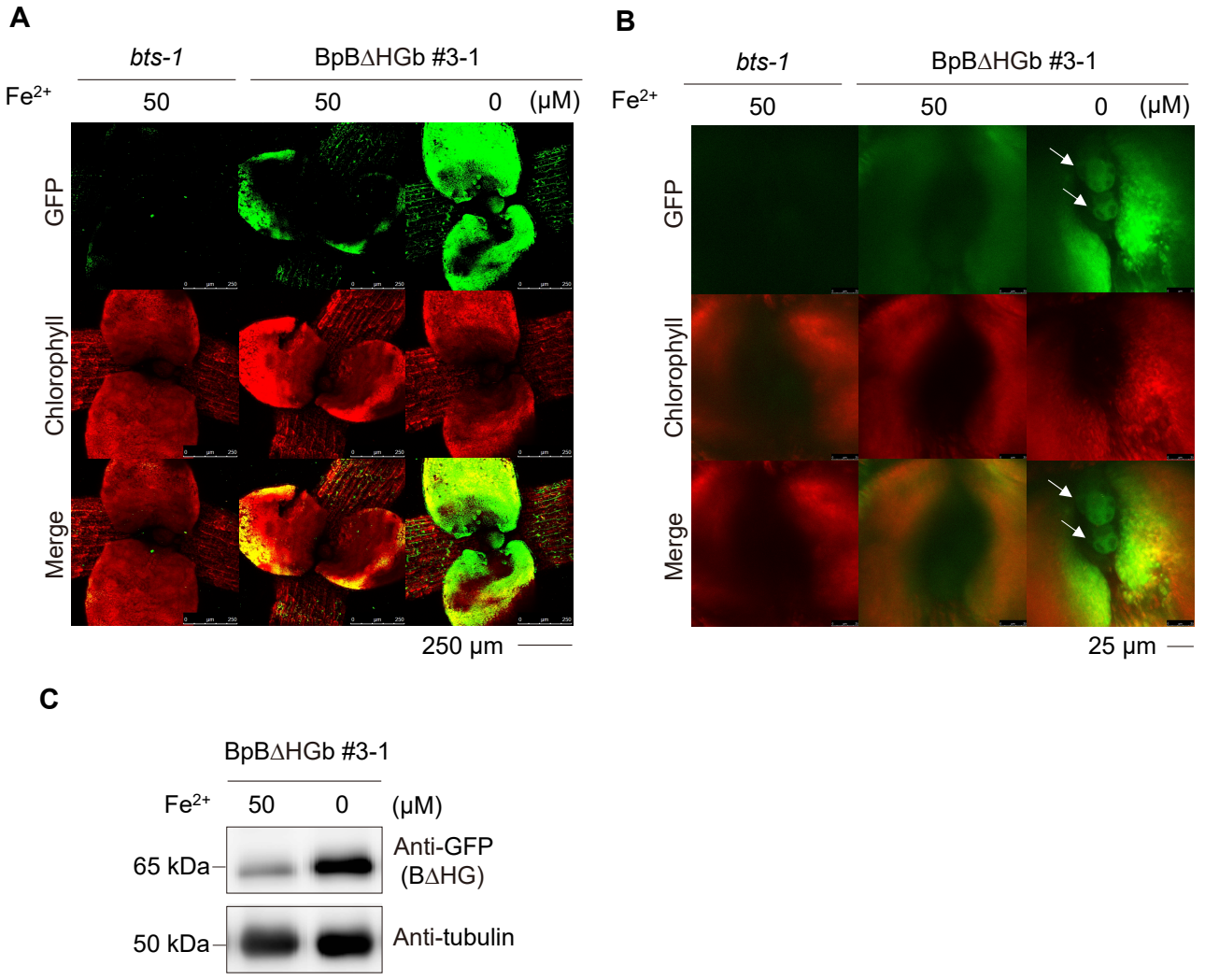

Fig. 1. The expression of *BTS* in leaf tissue is strongly induced under the iron deficiency condition. (A and B) Spatio-temporal expression pattern of *BΔHG* in leaf tissues. Three-day-old plants were transferred to iron depletion plates (0 μM Fe^{2+}) or normal plates (50 μM Fe^{2+}) and grown for 2 additional days. Images represent top-view GFP signals in plants obtained using a two-photon fluorescent microscope. 250× image (A); 1,000× image (B); green, GFP signal; red, chlorophyll autofluorescence. White arrows indicate newly emerging leaves. (C) Western blot analysis of the BΔHG protein level. Three-day-old plants were transferred and further grown on iron depletion plates (0 μM Fe^{2+}) or normal plates (50 μM Fe^{2+}) for 2 additional days. Protein extracts were analyzed by western blotting using anti-GFP antibody. Tubulin B was detected as loading control.

was detected at a low level under normal growth conditions but at a much higher level during iron deficiency. These results confirmed that the expression of *BTS* responds to iron deficiency in leaf tissues.

The *BTS-1* mutation causes up-regulation of genes related to photosynthesis and energy metabolism in shoot tissues

To gain insight into the role of BTS in the shoot, we performed RNA sequencing analysis of total RNA from the shoot tissue of Col-0 (wild-type) and *bts-1* plants. By comparing mRNA expression profiles of Col-0 and *bts-1* shoots, we identified 1,410 up-regulated and 1,748 down-regulated genes in *bts-1* shoots, compared with Col-0 shoots (Fig. 2A). The enrichment analysis of GOBPs revealed that the upregulated genes (DEGs) were mainly associated with photosynthesis, the respiratory electron transport chain (RETC), the ribonucleotide metabolic process (RMP), oxidative phosphorylation (OP), and iron homeostasis (Fig. 2B, red). In contrast, the down-regulated genes were associated with responses to ABA, osmotic stress, pathogens, and reactive oxygen species (ROS) (Fig. 2B, green).

We identified the processes where the *BTS-1* mutation had a dominant effect in shoot tissues by comparing the up- and down-regulated genes between shoot and root tissues. We also obtained a previously reported mRNA expression dataset generated from the root tissues of Col-0 and *bts-3* plants and identified 770 up-regulated and 885 down-regulated genes in *bts-3* roots, compared with Col-0 roots (Hindt et

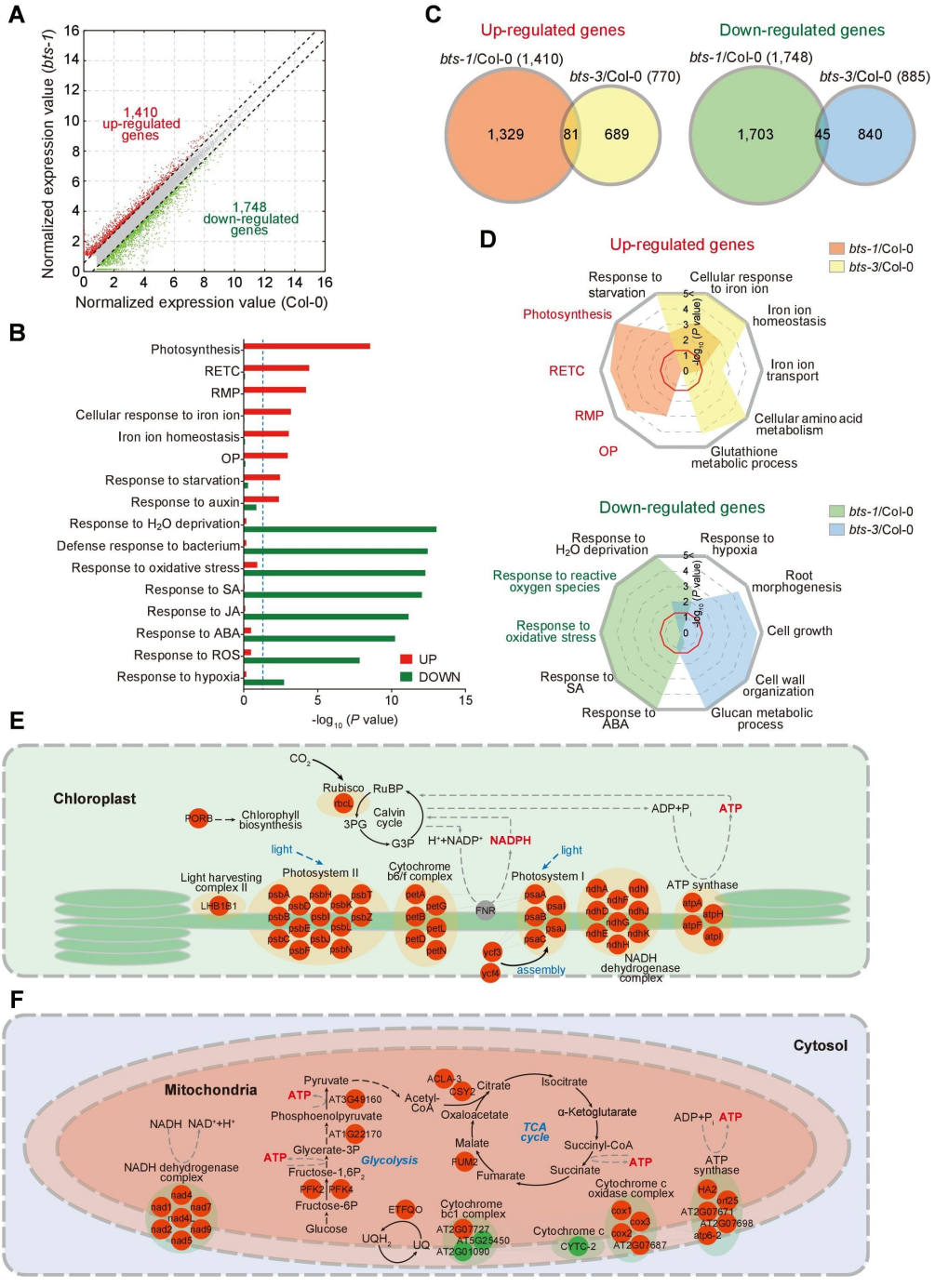

Fig. 2. Photosynthesis and energy metabolism-related genes are up-regulated in *bts-1* shoot tissues compared with Col-0 shoot tissues. (A) Scatter plot showing normalized expression levels of genes in Col-0 and *bts-1* shoot tissues. Up- and down-regulated genes are highlighted in red and green, respectively. (B) Bar graph showing GOBPs represented by up- (red) and down-regulated (green) genes in *bts-1* plants, compared with Col-0 plants. The significance (*P* value) of the GOBPs being enriched by the up- and down-regulated genes is displayed as -$\log_{10}$(*P* value). The cutoff of *P* value = 0.05 is indicated by a blue dashed line. (C) Venn diagrams describing relationships of up- (left) and down-regulated genes (right) between shoot (*bts-1*/Col-0) and root (*bts-3*/Col-0) tissues. The numbers of up- or down-regulated genes are denoted in parenthesis. (D) Radar plots showing GOBPs represented by up- (top) and down-regulated genes (bottom) in shoot (*bts-1*/Col-0) or root (*bts-3*/Col-0) tissues. The significance (*P* value) of the GOBPs being enriched by the up- and down-regulated genes is displayed as -$\log_{10}$(*P* value). The cutoff of *P* value = 0.05 is indicated by a red line. (E and F) Network models describing interactions among the up- (red) and down-regulated (green) genes involved in photosynthesis (E) and energy metabolism (F). Gray nodes indicate genes that are not affected by *BTS*, but added to the network to increase the connections among the nodes. Black solid/dashed arrows, direct/indirect activations; gray lines, protein-protein interactions; thick gray dashed lines, membrane.

al., 2017). The *bts-3* plants contain a single point mutation in the amino acid position 1174 from Pro to Leu at the RING domain of BTS. Only small proportion of the up- (5.74% of 1,410) and down-regulated (2.57% of 1,748) genes overlapped between shoot and root tissues (Fig. 2C), confirming that there is a little overlap in the genes regulated by BTS between shoot and root tissues. Genes related to most of the photosynthesis, RETC, RMP, and OP were up-regulated only in shoot tissues, while genes related to iron homeostasis and response to starvation were up-regulated in both shoot and root tissues (Fig. 2D, top). Responses to oxidative stress, ABA, and ROS were down-regulated only in shoot tissues, while responses to water deprivation and hypoxia were down-regulated in both shoot and root tissues (Fig. 2D, bottom). Among the processes affected by the *BTS-1* mutation, we focused on the shoot-specific and up-regulated processes: photosynthesis and energy metabolism. Network models describing interactions among the genes revealed close interactions among the up-regulated genes (Figs. 2E and 2F) in key pathways of photosynthesis and energy metabolism (photosystem complexes and glycolysis/TCA cycle), suggesting strong modulation of these processes by BTS.

We noted that the expression of a significant number of genes encoded in chloroplast and mitochondrial genomes was increased in *bts-1* shoots. These included the genes encoding key subunits for ATP and NADPH production (Leister, 2005). We selected several representative genes and examined their differential expression in *bts-1* and Col-0 shoots by qRT-PCR. The expression of chloroplast ATP synthase subunits (*atpA, atpF, atpH,* and *atpI*), the NADPH dehydrogenase subunits (*ndhA, ndhE, ndhI,* and *ndhK*), and genes involved in electron transport (*petB, petD, ycf3,* and *psbH*) were increased more than two-fold in *bts-1* shoot tissues compared with that in Col-0 shoot tissues (Fig. 3A). In addition, we also examined a few of the photosynthesis-associated genes (*PhANGs*) encoded in the nuclear genome. *PORA* and *PORB* (encoding protochlorophyllide oxidoreductase A and B, respectively) and *LHB1B1* (one of the genes constituting the light harvesting complex) were also expressed at higher levels in *bts-1* plants than in Col-0 plants (Supplementary Fig. S2B). Among mitochondrial genome-encoded genes, we also discovered that the expression of *cox1* and *cox3* (cytochrome oxidases 1 and 3, respectively), *nad4* and *nad4L* (NADPH dehydrogenase subunits 4 and 4 L, respectively), and *atpalpha, atpcfam, orf25, atp6-1,* and *atp6-2* (ATP synthase subunits) was increased by more than two-fold compared with that in Col-0 shoots (Fig. 3B). These results confirm the higher expression of these genes in transcriptome analysis.

bts-1 shoots show a significant increase in NADPH/NADP$^+$ and ADP/ATP ratios

The results of transcriptome analysis showing that the genes involved in ATP synthesis or NADPH synthesis were expressed at higher levels in *bts-1* shoot tissues prompted us to mea-

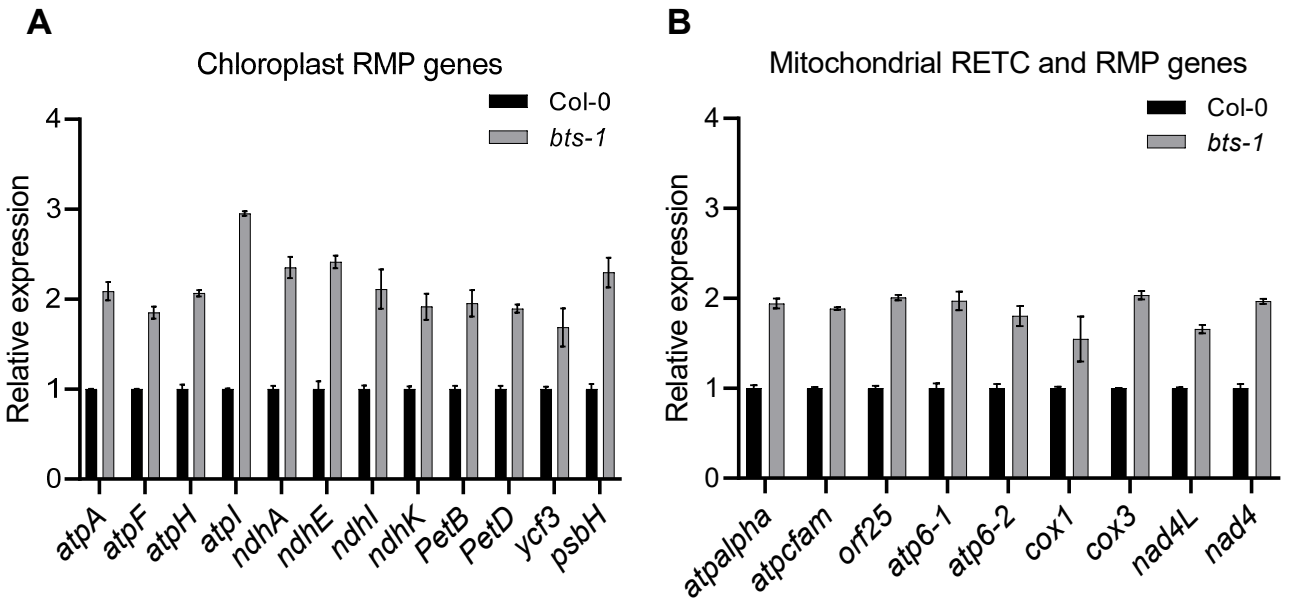

Fig. 3. Energy metabolism-related genes encoded in chloroplast and mitochondrial genomes are activated in shoot tissues in *bts-1* plants. (A) Relative transcript levels of energy metabolism-related genes encoded by the chloroplast genome. Total RNA was prepared from *bts-1* and Col-0 shoot tissues. The transcript levels were examined by qRT-PCR using gene-specific primers. The *16S rRNA* (chloroplast) transcript level was used as an internal control for the chloroplast gene expression. Relative fold expression of the indicated genes in *bts-1* plants were compared with Col-0 plants. Error bars indicate ± SD (n = 3). (B) Relative transcript levels of energy metabolism-related genes encoded in the mitochondrial genome. Total RNA was prepared from *bts-1* and Col-0 shoot tissues. The transcript levels were examined by qRT-PCR using gene-specific primers. The *ATMG00660* (encoded in the mitochondrial genome) transcript level was used as an internal control for the mitochondrial gene expression. Relative fold expression of the indicated genes in *bts-1* plants were compared with Col-0 plants. Error bars indicate ± SD (n = 3).

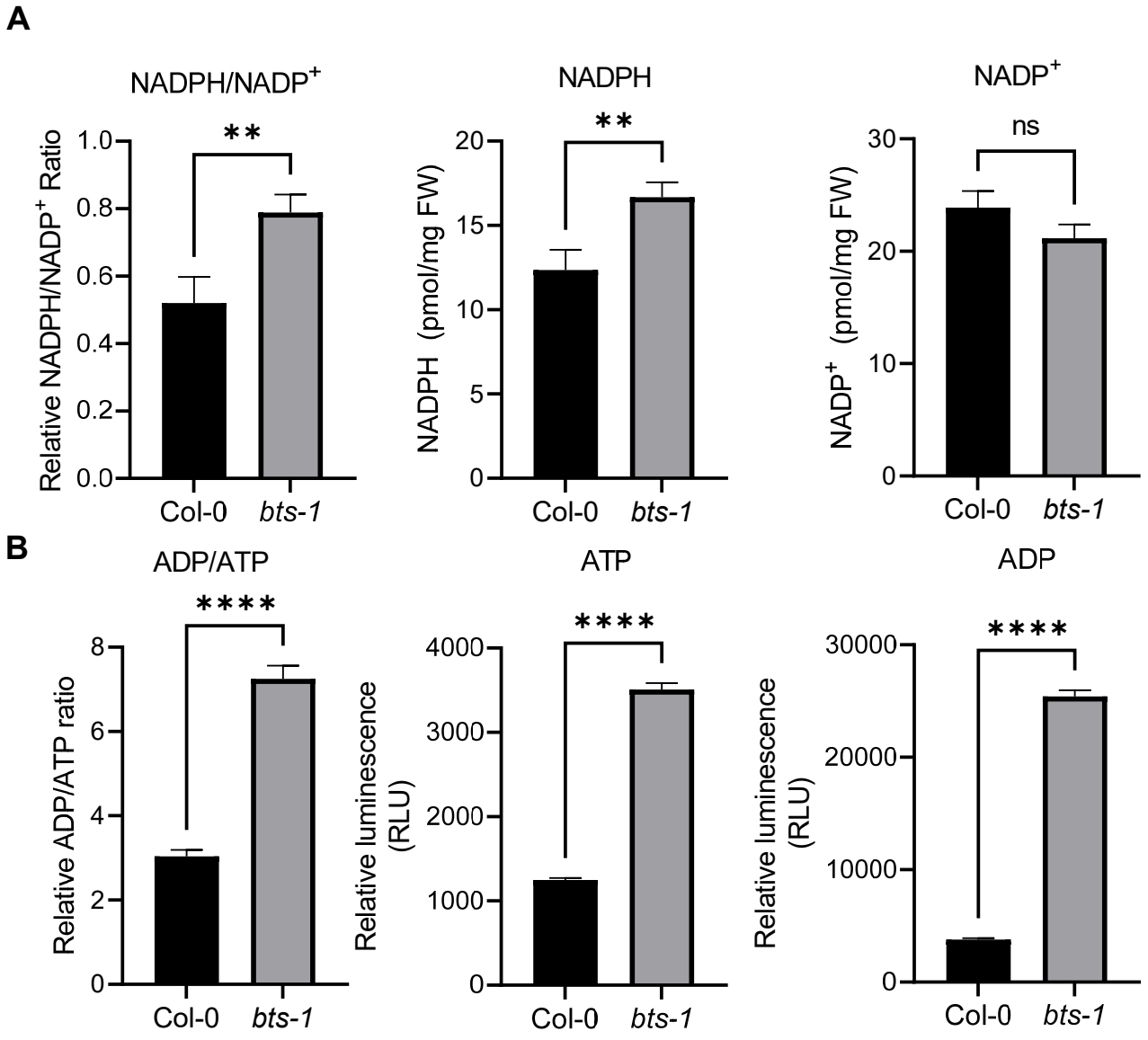

Fig. 4. NADPH/NADP$^+$ and ADP/ATP ratios are increased in shoot tissues in *bts-1* plants. (A) Measurement of NADPH and NADP$^+$ levels. The amount of NADPH and NADP$^+$ were measured from 10-day old plant shoot tissues using colorimetric detection kit. The amount of these compounds was calculated from the standard curve. Values are mean ± SD. Statistical analysis was carried out using Student's *t*-test. $^{**}P < 0.01$; ns, no significance (n = 3). (B) Effect of the *bts-1* mutation on the level of ATP and ADP. Extracts were prepared from 10-day old plant shoot tissues. ATP and ADP levels were measured using luminescence detection kit. RLU, relative light units. Values are mean ± SD. Statistical analysis was carried out using Student's *t*-test. $^{****}P < 0.0001$ (n = 3).

sure the levels of ATP, ADP, NADPH, and NADP$^+$ in *bts-1* shoot tissues. *bts-1* shoot tissues showed higher amounts of NADPH compared with Col-0 shoot tissues, thereby resulting in a higher ratio of NADPH/NADP$^+$ (Fig. 4A). In addition, *bts-1* shoot tissues showed nine- and three-fold higher levels of ADP and ATP, respectively, compared with Col-0 shoot tissues. Thus, the ADP/ATP ratio was three-fold higher in *bts-1* shoot tissues than Col-0 shoot tissues (Fig. 4B). The increased ADP level in *bts-1* shoot tissues raises the possibility that *bts-1* plants consume more ATP than Col-0 plants and, therefore, have a higher rate of energy metabolism.

bts-1 shoot tissues show an increase in values of ETR_{II} and Y_{II}, and chlorophyll contents, but a decrease in soluble sugar and starch contents

Transcriptome analysis showed that photosynthesis-related genes were expressed at higher levels in *bts-1* shoot tissues compared with Col-0 shoot tissues. To corroborate this finding at the physiological level, we examined whether the photosynthetic parameters were increased in the *bts-1* plant as well. In particular, iron in shoot tissues is important for electron transport chain reactions in chloroplasts. Moreover, it has been shown that *bts-1* plants have higher iron contents than Col-0 plants (Hindt et al., 2017; Selote et al., 2015). We

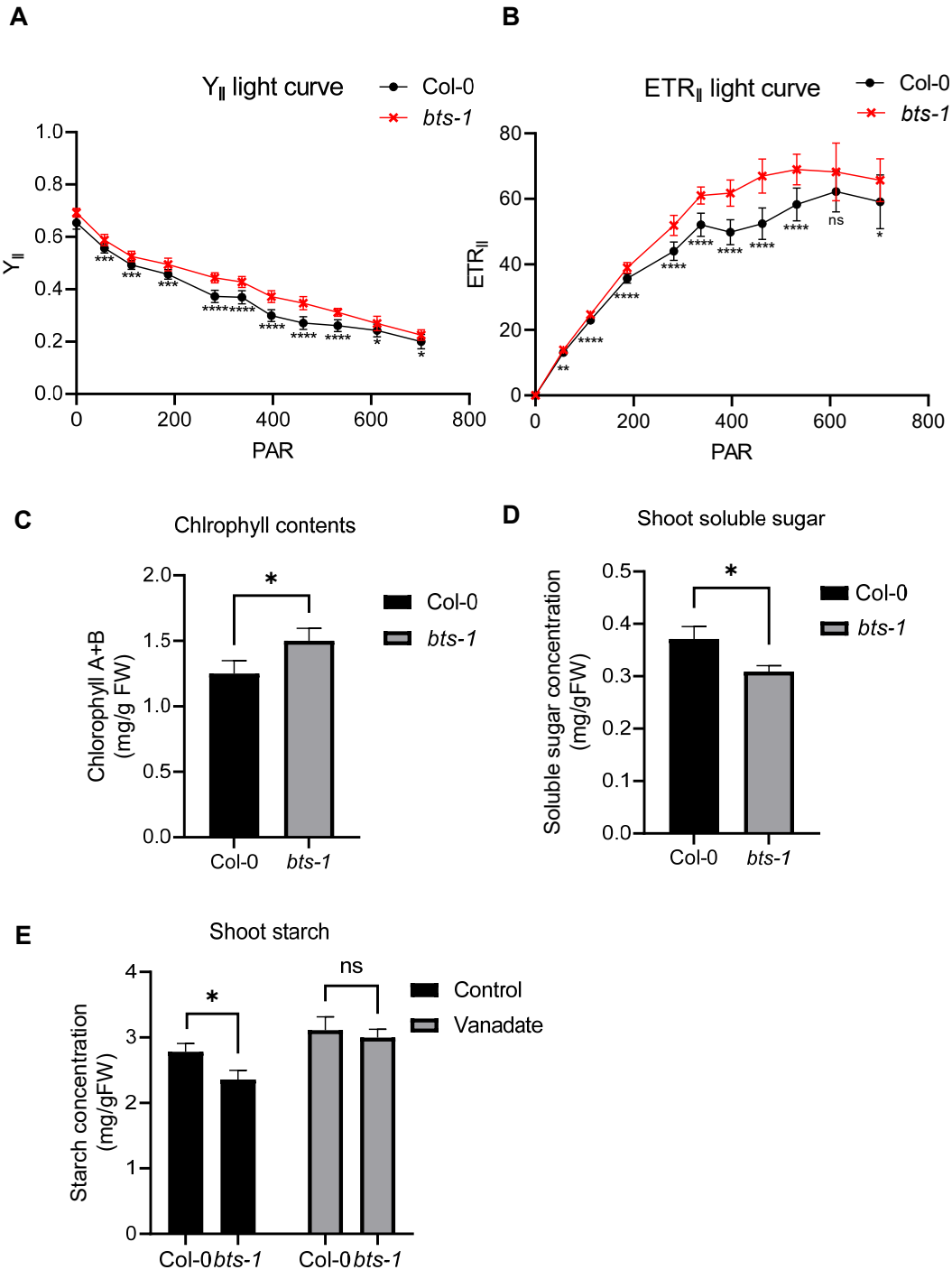

Fig. 5. *bts-1* shoot tissues show an increase in the values of Y_{II} and ETR_{II}, and chlorophyll contents, but a decrease in soluble sugar and starch contents. (A and B) Photosynthetic parameters of *bts-1* shoot tissues compared with Col-0 shoot tissues. Plants grown on normal plates were further grown at the indicated conditions for 7 days. Values of Y_{II} (A) and ETR_{II} (B) were measured with increasing PAR. Values are mean ± SD. Statistical analysis was performed using Student's *t*-test between *bts-1* and Col-0 plants. $*P < 0.05$; $**P < 0.01$; $***P < 0.001$; $****P < 0.0001$; ns, no significance (n = 13). (C) Measurement of chlorophyll A+B contents in *bts-1* plants compared with Col-0 plants. Values are mean ± SD. Statistical analysis was performed using Student's *t*-test. $*P < 0.05$ (n = 3). (D) Effect of the *BTS-1* mutation on soluble sugar contents in shoot tissues. Soluble sugars were measured from *bts-1* plant shoot tissues compared with Col-0 shoot tissues. Values are mean ± SD. Statistical analysis was performed using Student's *t*-test. $*P < 0.05$ (n = 3). (E) Effect of the *BTS-1* mutation and vanadate on starch contents in shoot tissues. Starch content were measured from shoot tissues of *bts-1* plants with or without treatment after 1 mM vanadate for 1 h and compared with shoot tissues of Col-0 plants. Values are mean ± SD. Statistical analysis was performed using Student's *t*-test. $*P < 0.05$; ns, no significance (n = 3).

measured electron transport rate (ETR_{II}) together with actual quantum yield (Y_{II}) (Kramer et al., 2004) along with increasing photosynthetically active radiation (PAR). *bts-1* plants showed an increase in the values of Y_{II} and ETR_{II} along with increasing PAR intensity of light, compared with Col-0 plants (Figs. 5A and 5B). Previous studies showed that a higher photosynthetic efficiency is closely correlated with higher chlorophyll contents (Gratani et al., 1998; Lin et al., 2011). Thus, we measured chlorophyll levels of *bts-1* plants. In agreement with the higher values of Y_{II} and ETR_{II}, *bts-1* plants showed an increase in the chlorophyll levels compared with Col-0 plants (Fig. 5C). The data suggested that *bts-1* plants use more light in photochemical reactions, such as the production of high-energy electrons, and transfer more electrons at a given time compared with Col-0 plants.

Plants accumulate starch in the chloroplast during the day, through photosynthesis in the chloroplast, and transport sucrose, another carbon source, to sink tissues through the phloem (Hennion et al., 2019; Lemoine et al., 2013). Since *bts-1* plants exhibit increased photosynthetic parameters, we reasoned that they might also exhibit an increase in starch and soluble sugar content in the shoot. Thus, we examined their levels in both *bts-1* and Col-0 shoot tissues. In contrast to the photosynthetic parameters, the amounts of starch and soluble sugar were lower in *bts-1* shoot tissues than in Col-0 shoot tissues (Figs. 5D and 5E), raising the possibility that *bts-1* plants have a process that consumes a large amount of energy. Indeed, this idea is consistent with the fact that the level of ADP was greatly increased in *bts-1* shoot tissues compared with Col-0 shoot tissues. A previous study showed that *bts-1* plants show a strong rhizosphere acidification (Selote et al., 2015). For rhizosphere acidification, H^+-ATPases at the plasma membrane pump out H^+ via ATP hydrolysis (Duby and Boutry, 2009; Kumar et al., 2006; Niittylä et al., 2007; Okumura et al., 2016). Thus, for strong acidification of the rhizosphere, a photosynthetically fixed carbon source should be transported from the shoot tissue to the root tissue where a large amount of ATP can be generated. It has been shown that the activation of H^+-ATPases is also critical for protons to be released to the rhizosphere (Oh et al., 2016; Santi and Schmidt, 2009). Thus, one possibility is that *bts-1* plants use carbohydrates for rhizosphere acidification. Thus *bts-1* plants may not be able to accumulate starch in leaf tissues even though photosynthesis-related processes occur at higher rates. To test this idea, we examined whether starch levels return to normal levels in *bts-1* shoot tissues when H^+-ATPase is inhibited. We treated *bts-1* plants with vanadate, an inhibitor of H^+-ATPase (Falhof et al., 2016; O'Neill and Spanswick, 1984) for 1 h and examined the amount of starch. The starch content in *bts-1* shoot tissues was the same of that in Col-0 shoot tissues (Fig. 5E), indicating that a large amount of starch was used for rhizosphere acidification through hydrolysis of ATP by plasma membrane H^+-ATPases.

DISCUSSION

While BTS is known to play a critical role in iron deficiency response in root tissue, here we focused on the function of BTS in shoot tissue. In iron homeostasis, iron-related processes may primarily concern the uptake of iron from soil. Thus, it has been suggested that BTS plays a role in preventing the uptake of excess iron from the soil. However, iron-homeostasis-related processes in leaf tissues may primarily concern the distribution of iron that arrives from root tissues. Thus, the role of BTS in iron homeostasis in leaf tissues, if any, may be different from that in root tissues.

A previous study showed that the knock-out mutation of *BTS* is lethal (McElver et al., 2001; Selote et al., 2015; Tzafrir et al., 2004). This result raises the possibility that BTS plays a role in various developmental stages. In a previous study, transcriptional GUS fusion was used to visualize the spatio-temporal expression of *BTS*. Indeed, *BTS* is expressed in various tissues and at various time points during plant development (Selote et al., 2015). Here, we used translational fusion of GFP-tagged reporter BΔHG under the control of the BTS native promoter. GFP has been widely used to study the spatio-temporal expression pattern of genes (Chiu et al., 1996). The GFP expression study revealed that *BTS* was expressed at the margin of true leaves but not cotyledon under normal growth conditions. During iron deficiency, the expression of *GFP* occurred much more broadly in the entire leaf tissue and also in the newly emerging leaves, suggesting that iron deficiency response regulates the *BTS* expression in shoot tissues, similar to root tissues (Hindt et al., 2017; Selote et al., 2015). Iron cannot be remobilized from mature leaves. Thus, during iron deficiency, Fe is unable to be transported from the older shoot tissue to younger shoot tissue (Zhang et al., 1996). This is consistent with our results that iron-deficiency-induced *BTS* expression occurs largely in newly produced cells in emerging leaves. However, our GFP-based expression pattern was slightly different from the previous data based on the expression pattern of *GUS* under the *BTS* promoter (Selote et al., 2015). The earlier study showed that *BTS* is highly expressed in young leaves but only in veins in old leaves. However, our data showed that *BΔHG* expresses only in leaf margins under normal growth conditions but in the entire leaf during iron deficiency. We used translational fusion with a more stabilized version of BTS (BΔH), which may account for differences in the expression pattern from the earlier study.

In shoot tissues, iron plays a crucial role as a cofactor in the form of Fe-S cluster or heme for proteins involved in the electron transport chain reaction of the energy production process and many other processes (Kroh and Pilon, 2020). Thus, one possibility is that BTS is negatively involved in the assimilation of iron into key metabolic enzymes in young leaves. Shoot transcriptome analysis of *bts-1* plants supports this notion; *bts-1* plants showed significant increases in the expression of genes involved in photosynthesis and energy metabolism. Moreover, many up-regulated genes were encoded by the two organellar genomes: chloroplast and mitochondrial genomes. This was rather unexpected because BTS has not been shown to play a role in organellar function in root tissues. Currently, the mechanism by which BTS plays a role in regulation of organellar genes is not clearly understood. This result strongly suggests that the biological role of BTS in leaf tissues is different from that in root tissues.

More than 80% of the chloroplast gene expression was

transcribed by plastid-encoded RNA polymerase (PEP) and the remainder by nucleus-encoded RNA polymerase (PAP) (Zhang et al., 2020). PEP works in a complex with PAPs. Mitochondrial gene expression is regulated through various proteins with DNA-binding or RNA-binding motifs (Lee et al., 2012a; Narsai et al., 2011; Shevtsov et al., 2018). Recently, the mitochondrial transcription termination factor (mTERF) family has been studied for its important function in regulating mitochondrial expression (Shevtsov et al., 2018). However, currently, it is not clearly understood how a lower expression level of BTS leads to up-regulation of these genes encoded by the organellar genomes. Possibly, among many target substrates of BTS, there should be transcription factors or transcription-related factors that control the genes involved in the processes.

Consistent with the higher expression of genes involved in photosynthesis in *bts-1* shoot tissues compared with Col-0 shoot tissues, the values of ETR_{II} and Y_{II} were higher in *bts-1* plant shoots than Col-0 shoot tissues. Chlorophyll levels of *bts-1* plants were increased as well. Furthermore, the production of ATP and NADPH in *bts-1* shoot tissues was higher than Col-0 shoot tissues. This was also consistent with the higher expression of genes involved in ATP production in *bts-1* shoot tissues than in Col-0 shoot tissues (Figs. 2 and 3). These results suggest that BTS is involved in not only regulation of the iron content as a negative regulator but also is negatively involved in energy metabolism, such as the production of ATP. However, it is seemingly contradictory that *bts-1* plants have a high energy demand but at the same time have higher ATP levels compared with wild-type plants. Perhaps feedback regulation is taking place to supplement the high energy demand in *bts-1* plants. One intriguing aspect is the ratio of ADP/ATP, which was three-fold higher in *bts-1* shoot tissues than Col-0 shoot tissues. This raises the possibility that ATP consumption increases even further than the increase in ATP production. Consistent with this, *bts-1* plants showed lower levels of soluble sugar and starch than Col-0 plants. Chloroplasts and mitochondria provide the energy source necessary for cells (Allen, 2015). When cellular energy demands increase, the expression of chloroplast and mitochondrial genes involved in ATP production increases (Allen, 2015; Shevtsov et al., 2018; Zhang et al., 2020). Thus, the increase in the expression of energy-metabolism-related organellar genes suggests that *bts-1* plants have high energy demands. Indeed, *bts-1* plants showed a strong rhizosphere acidification, which requires a high amount of ATP (Oh et al., 2016; Palmgren, 2001; Santi and Schmidt, 2009). In addition, the uptake, movement and storage of iron in plants are also energy demanding processes that use ATP (Shameer et al., 2018; Yan et al., 2002). This is consistent with the finding that the starch content of *bts-1* shoot tissues was restored to normal levels upon the treatment with vanadate, an inhibitor of H^+-ATPases.

In conclusion, we provide evidence that BTS plays an important role in various cellular processes in negative manners. While it negatively regulates iron deficiency responses in the root tissue, it is involved in suppression of genes involved in energy-metabolism-related processes in shoot tissue, suppressing energy metabolism in shoot tissue. In the future, further studies will be necessary to explore the mechanism by which BTS regulates the expression of genes that concern energy-metabolism-related processes in shoot tissue.

Note: Supplementary information is available on the Molecules and Cells website (www.molcells.org).

ACKNOWLEDGMENTS

This work was supported by the National Research Foundation of Korea (NRF) and funded by a grant from the Korea government (MSIT) (No. 2019R1A2B5B03099982).

AUTHOR CONTRIBUTIONS

B.C. and D.Y.H. performed the experiments and wrote the primary manuscript. I.H. and D.H. designed and supervised the study. T.A.L. and J.L. contributed to the data analysis and revision of the manuscript.

CONFLICT OF INTEREST

The authors have no potential conflicts of interest to disclose.

ORCID

Bongsoo Choi https://orcid.org/0000-0001-8869-4200
Do Young Hyeon https://orcid.org/0000-0002-6870-4827
Juhun Lee https://orcid.org/0000-0003-2749-8665
Terri A. Long https://orcid.org/0000-0001-7846-0195
Daehee Hwang https://orcid.org/0000-0002-7553-0044
Inhwan Hwang https://orcid.org/0000-0002-1388-1367

REFERENCES

Allen, J.F. (2015). Why chloroplasts and mitochondria retain their own genomes and genetic systems: colocation for redox regulation of gene expression. Proc. Natl. Acad. Sci. U. S. A. *112*, 10231-10238.

Anders, S., Pyl, P.T., and Huber, W. (2015). HTSeq--a Python framework to work with high-throughput sequencing data. Bioinformatics *31*, 166-169.

Bolstad, B.M., Irizarry, R.A., Astrand, M., and Speed, T.P. (2003). A comparison of normalization methods for high density oligonucleotide array data based on variance and bias. Bioinformatics *19*, 185-193.

Chiu, W.L., Niwa, Y., Zeng, W., Hirano, T., Kobayashi, H., and Sheen, J. (1996). Engineered GFP as a vital reporter in plants. Curr. Biol. *6*, 325-330.

Clough, S.J. and Bent, A.F. (1998). Floral dip: a simplified method for Agrobacterium-mediated transformation of Arabidopsis thaliana. Plant J. *16*, 735-743.

Duby, G. and Boutry, M. (2009). The plant plasma membrane proton pump ATPase: a highly regulated P-type ATPase with multiple physiological roles. Pflugers Arch. *457*, 645-655.

Enomoto, Y., Hodoshima, H., Shimada, H., Shoji, K., Yoshihara, T., and Goto, F. (2007). Long-distance signals positively regulate the expression of iron uptake genes in tobacco roots. Planta *227*, 81-89.

Falhof, J., Pedersen, J.T., Fuglsang, A.T., and Palmgren, M. (2016). Plasma membrane H(+)-ATPase regulation in the center of plant physiology. Mol. Plant *9*, 323-337.

García, M.J., Romera, F.J., Stacey, M.G., Stacey, G., Villar, E., Alcántara, E., and Pérez-Vicente, R. (2013). Shoot to root communication is necessary to control the expression of iron-acquisition genes in Strategy I plants. Planta *237*, 65-75.

Gratani, L., Pesoli, P., and Crescente, M.F. (1998). Relationship between photosynthetic activity and chlorophyll content in an isolated Quercus ilex L. tree during the year. Photosynthetica *35*, 445-451.

Grillet, L., Lan, P., Li, W., Mokkapati, G., and Schmidt, W. (2018). IRON MAN

is a ubiquitous family of peptides that control iron transport in plants. Nat. Plants *4*, 953-963.

Hennion, N., Durand, M., Vriet, C., Doidy, J., Maurousset, L., Lemoine, R., and Pourtau, N. (2019). Sugars en route to the roots. Transport, metabolism and storage within plant roots and towards microorganisms of the rhizosphere. Physiol. Plant. *165*, 44-57.

Hindt, M.N., Akmakjian, G.Z., Pivarski, K.L., Punshon, T., Baxter, I., Salt, D.E., and Guerinot, M.L. (2017). BRUTUS and its paralogs, BTS LIKE1 and BTS LIKE2, encode important negative regulators of the iron deficiency response in Arabidopsis thaliana. Metallomics *9*, 876-890.

Hossain, M.A., Kamiya, T., Burritt, D.J., Phan Tran, L.S., and Fujiwara, T. (2018). Plant Micronutrient Use Efficiency: Molecular and Genomic Perspectives in Crop Plants (San Diego: Elsevier Science & Technology).

Huang, D.W., Sherman, B.T., and Lempicki, R.A. (2009). Systematic and integrative analysis of large gene lists using DAVID bioinformatics resources. Nat. Protoc. *4*, 44-57.

Kaplan, J. and Ward, D.M. (2013). The essential nature of iron usage and regulation. Curr. Biol. *23*, R642-R646.

Kobayashi, T. and Nishizawa, N.K. (2012). Iron uptake, translocation, and regulation in higher plants. Annu. Rev. Plant Biol. *63*, 131-152.

Kobayashi, T. and Nishizawa, N.K. (2014). Iron sensors and signals in response to iron deficiency. Plant Sci. *224*, 36-43.

Kobayashi, T., Nozoye, T., and Nishizawa, N.K. (2019). Iron transport and its regulation in plants. Free Radic. Biol. Med. *133*, 11-20.

Kramer, D.M., Johnson, G., Kiirats, O., and Edwards, G.E. (2004). New fluorescence parameters for the determination of QA redox state and excitation energy fluxes. Photosynth. Res. *79*, 209.

Kroh, G.E. and Pilon, M. (2019). Connecting the negatives and positives of plant iron homeostasis. New Phytol. *223*, 1052-1055.

Kroh, G.E. and Pilon, M. (2020). Regulation of iron homeostasis and use in chloroplasts. Int. J. Mol. Sci. *21*, 3395.

Kumar, R., Pandey, S., and Pandey, A. (2006). Plant roots and carbon sequestration. Curr. Sci. *91*, 885-890.

Lee, C.P., Eubel, H., Solheim, C., and Millar, A.H. (2012a). Mitochondrial proteome heterogeneity between tissues from the vegetative and reproductive stages of Arabidopsis thaliana development. J. Proteome Res. *11*, 3326-3343.

Lee, J., Choi, B., Yun, A., Son, N., Ahn, G., Cha, J.Y., Kim, W.Y., and Hwang, I. (2021). Long-term abscisic acid promotes golden2-like1 degradation through constitutive photomorphogenic 1 in a light intensity-dependent manner to suppress chloroplast development. Plant Cell Environ. *44*, 3034-3048.

Lee, S., Kim, Y.S., Jeon, U.S., Kim, Y.K., Schjoerring, J.K., and An, G. (2012b). Activation of rice nicotianamine synthase 2 (OsNAS2) enhances iron availability for biofortification. Mol. Cells *33*, 269-275.

Leister, D. (2005). Genomics-based dissection of the cross-talk of chloroplasts with the nucleus and mitochondria in Arabidopsis. Gene *354*, 110-116.

Lemoine, R., La Camera, S., Atanassova, R., Dédaldéchamp, F., Allario, T., Pourtau, N., Bonnemain, J.L., Laloi, M., Coutos-Thévenot, P., Maurousset, L., et al. (2013). Source-to-sink transport of sugar and regulation by environmental factors. Front. Plant Sci. *4*, 272.

Li, Z., Wu, Y., Xing, D., Zhang, K., Xie, J., Yu, R., Chen, T., and Duan, R. (2021). Effects of foliage spraying with sodium bisulfite on the photosynthesis of Orychophragmus violaceus. Horticulturae *7*, 137.

Lin, A., Shen, S., Wang, G., Yi, Q., Qiao, H., Niu, J., and Pan, G. (2011). Comparison of chlorophyll and photosynthesis parameters of floating and attached Ulva prolifera. J. Integr. Plant Biol. *53*, 25-34.

Long, T.A., Tsukagoshi, H., Busch, W., Lahner, B., Salt, D.E., and Benfey, P.N. (2010). The bHLH transcription factor POPEYE regulates response to iron deficiency in Arabidopsis roots. Plant Cell *22*, 2219-2236.

Martin, M. (2011). Cutadapt removes adapter sequences from high-throughput sequencing reads. EMBnet J. *17*, 10-12.

McElver, J., Tzafrir, I., Aux, G., Rogers, R., Ashby, C., Smith, K., Thomas, C., Schetter, A., Zhou, Q., Cushman, M.A., et al. (2001). Insertional mutagenesis of genes required for seed development in Arabidopsis thaliana. Genetics *159*, 1751-1763.

Mendoza-Cózatl, D.G., Xie, Q., Akmakjian, G.Z., Jobe, T.O., Patel, A., Stacey, M.G., Song, L., Demoin, D.W., Jurisson, S.S., Stacey, G., et al. (2014). OPT3 is a component of the iron-signaling network between leaves and roots and misregulation of OPT3 leads to an over-accumulation of cadmium in seeds. Mol. Plant *7*, 1455-1469.

Narsai, R., Law, S.R., Carrie, C., Xu, L., and Whelan, J. (2011). In-depth temporal transcriptome profiling reveals a crucial developmental switch with roles for RNA processing and organelle metabolism that are essential for germination in Arabidopsis. Plant Physiol. *157*, 1342-1362.

Niittylä, T., Fuglsang, A.T., Palmgren, M.G., Frommer, W.B., and Schulze, W.X. (2007). Temporal analysis of sucrose-induced phosphorylation changes in plasma membrane proteins of Arabidopsis. Mol. Cell. Proteomics *6*, 1711-1726.

O'Neill, S.D. and Spanswick, R.M. (1984). Effects of vanadate on the plasma membrane ATPase of red beet and corn. Plant Physiol. *75*, 586-591.

Oh, Y.J., Kim, H., Seo, S.H., Hwang, B.G., Chang, Y.S., Lee, J., Lee, D.W., Sohn, E.J., Lee, S.J., Lee, Y., et al. (2016). Cytochrome b 5 reductase 1 triggers serial reactions that lead to iron uptake in plants. Mol. Plant *9*, 501-513.

Okumura, M., Inoue, S.I., Kuwata, K., and Kinoshita, T. (2016). Photosynthesis activates plasma membrane H+-ATPase via sugar accumulation. Plant Physiol. *171*, 580-589.

Palmgren, M.G. (2001). Plant plasma membrane H+-ATPases: powerhouses for nutrient uptake. Annu. Rev. Plant Physiol. Plant Mol. Biol. *52*, 817-845.

Rodriguez-Celma, J., Connorton, J.M., Kruse, I., Green, R.T., Franceschetti, M., Chen, Y.T., Cui, Y., Ling, H.Q., Yeh, K.C., and Balk, J. (2019). Arabidopsis BRUTUS-LIKE E3 ligases negatively regulate iron uptake by targeting transcription factor FIT for recycling. Proc. Natl. Acad. Sci. U. S. A. *116*, 17584-17591.

Santi, S. and Schmidt, W. (2009). Dissecting iron deficiency-induced proton extrusion in Arabidopsis roots. New Phytol. *183*, 1072-1084.

Selote, D., Samira, R., Matthiadis, A., Gillikin, J.W., and Long, T.A. (2015). Iron-binding E3 ligase mediates iron response in plants by targeting basic helix-loop-helix transcription factors. Plant Physiol. *167*, 273-286.

Shameer, S., Baghalian, K., Cheung, C.Y.M., Ratcliffe, R.G., and Sweetlove, L.J. (2018). Computational analysis of the productivity potential of CAM. Nat. Plants *4*, 165-171.

Shevtsov, S., Nevo-Dinur, K., Faigon, L., Sultan, L.D., Zmudjak, M., Markovits, M., and Ostersetzer-Biran, O. (2018). Control of organelle gene expression by the mitochondrial transcription termination factor mTERF22 in Arabidopsis thaliana plants. PLoS One *13*, e0201631.

Trapnell, C., Pachter, L., and Salzberg, S.L. (2009). TopHat: discovering splice junctions with RNA-Seq. Bioinformatics *25*, 1105-1111.

Tzafrir, I., Pena-Muralla, R., Dickerman, A., Berg, M., Rogers, R., Hutchens, S., Sweeney, T.C., McElver, J., Aux, G., Patton, D., et al. (2004). Identification of genes required for embryo development in Arabidopsis. Plant Physiol. *135*, 1206-1220.

Vert, G.G.A., Briat, J.F.O., and Curie, C. (2003). Dual regulation of the Arabidopsis high-affinity root iron uptake system by local and long-distance signals. Plant Physiol. *132*, 796-804.

Wang, M., Lee, J., Choi, B., Park, Y., Sim, H.J., Kim, H., and Hwang, I. (2018). Physiological and molecular processes associated with long duration of ABA treatment. Front. Plant Sci. *9*, 176.

Yan, F., Zhu, Y., Muller, C., Zorb, C., and Schubert, S. (2002). Adaptation of H+-pumping and plasma membrane H+ ATPase activity in proteoid roots of white lupin under phosphate deficiency. Plant Physiol. *129*, 50-63.

Zhang, C., Römheld, V., and Marschner, H. (1996). Remobilization of iron from primary leaves of bean plants grown at various iron levels. J. Plant Nutr. *19*, 1017-1028.

Zhang, Y., Zhang, A., Li, X., and Lu, C. (2020). The role of chloroplast gene expression in plant responses to environmental stress. Int. J. Mol. Sci. *21*, 6082.